Science Advances
AAAS

advances.sciencemag.org/cgi/content/full/5/11/eaaw5643/DC1

Supplementary Materials for

Supramolecular silicone coating capable of strong substrate bonding, readily damage healing, and easy oil sliding

Meijin Liu, Zhaoyue Wang, Peng Liu, Zuankai Wang, Haimin Yao, Xi Yao*

*Corresponding author. Email: xi.yao@cityu.edu.hk

Published 1 November 2019, *Sci. Adv.* **5**, eaaw5643 (2019)
DOI: 10.1126/sciadv.aaw5643

This PDF file includes:

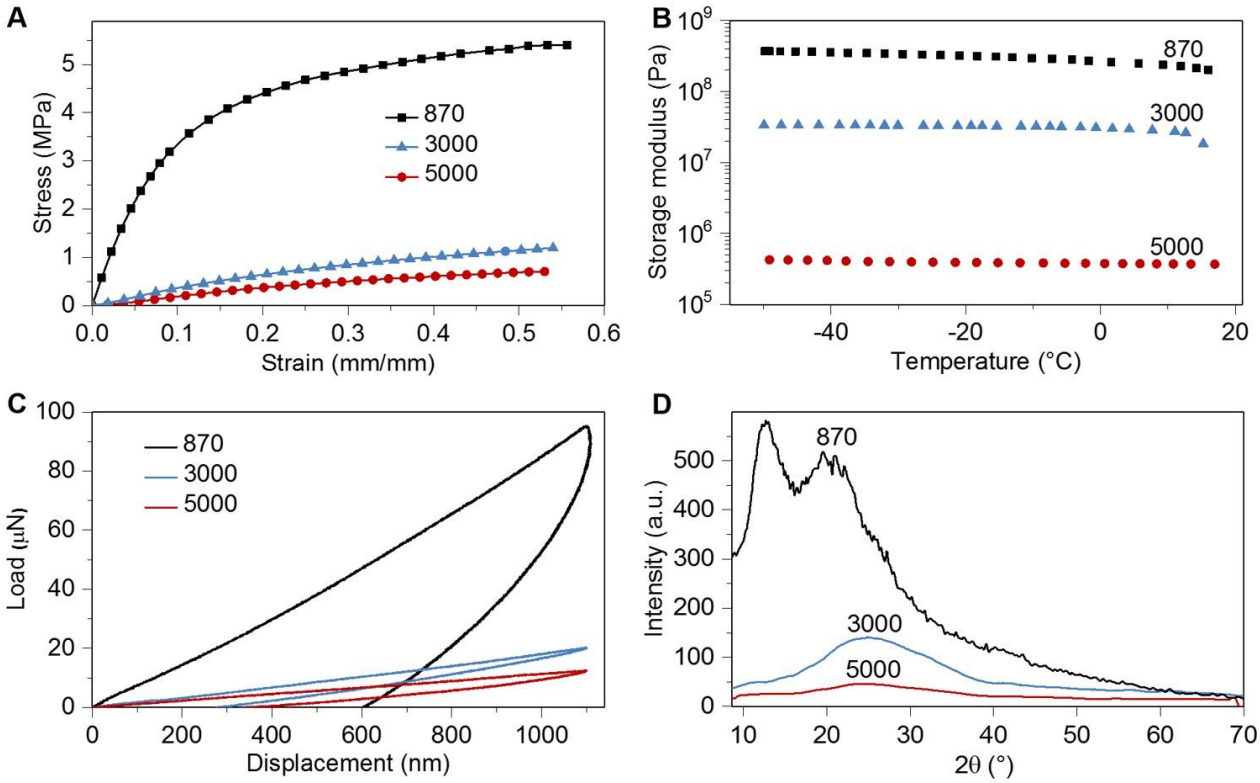

Fig. S1. Mechanical properties of siloxane oligomer materials with different MWs. (**A**) Tensile test curves, (**B**) representative dynamic mechanical analysis (DMA) traces, (**C**) indentation tests and (**D**) powder X-ray diffractogram of siloxane oligomer materials with different molecule weights. It is found that the mechanical properties of siloxane oligomer-based supramolecular polymers decrease exponentially with the growth of H_2N-PDMS-NH_2 molecular weight. Specifically, when changing the molecular weight from ~870 to ~3000 and ~5000, the Young's modulus by tensile testing decreases from ~47.39 ± 1.03 MPa to ~3.67 ± 0.32 MPa and ~2.11 ± 0.21 MPa (A), storage modulus at 0˚C by dynamic thermomechanical analysis (DMA) decreases from ~264.48 ± 13.91 MPa to ~30.67 ± 1.27 MPa and ~0.38 ± 0.06 MPa (B), and Young's modulus by indentation decreases from ~155.35 ± 10.27 MPa to ~11.79 ± 1.41 MPa and ~5.30 ± 0.29 MPa (C), respectively.

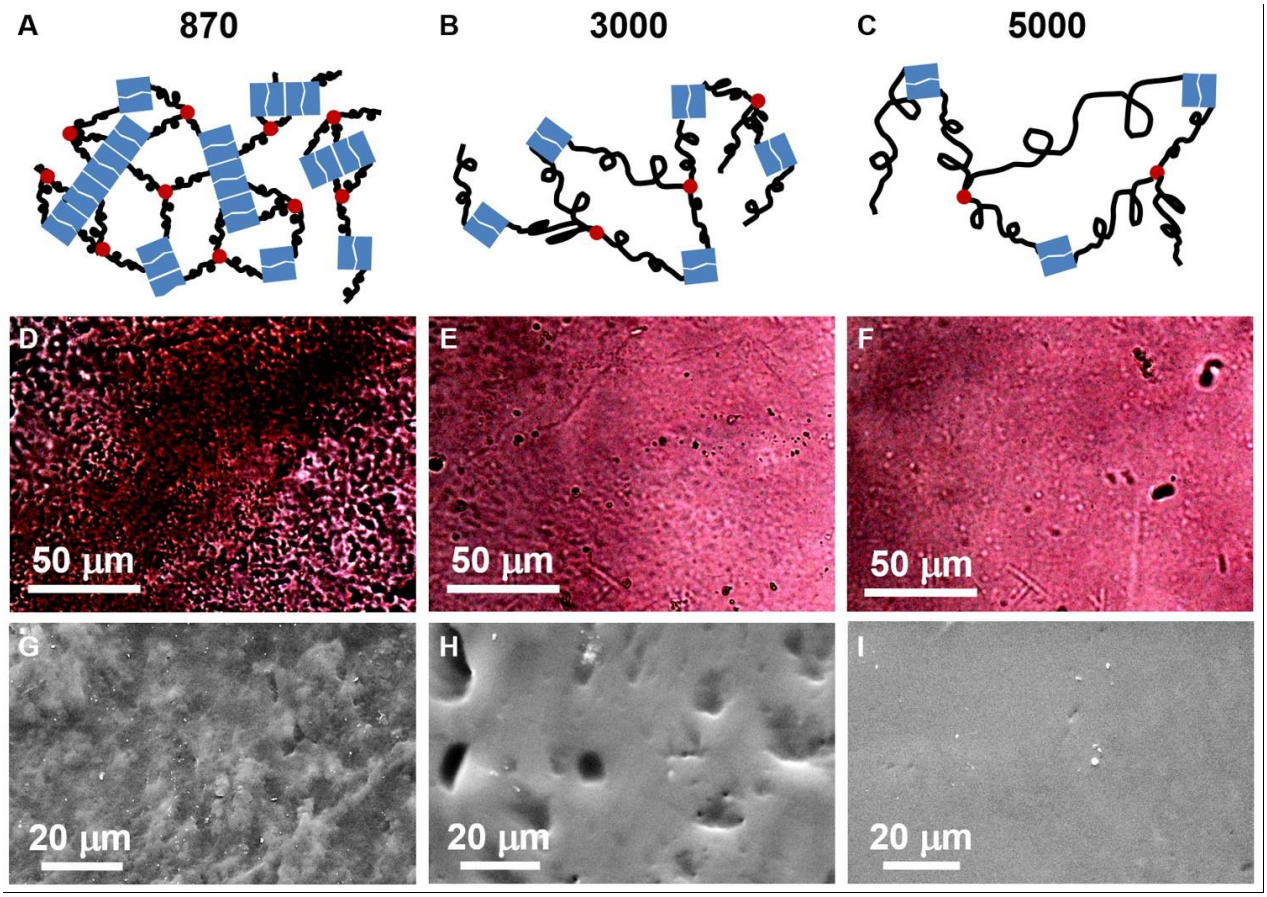

Fig. S2. Structures of siloxane oligomer materials with different MWs. Scheme, POM images and SEM images of interior sections illustrated the structures of siloxane oligomer materials with molecule weights of ~870 (**A**, **D** and **G**), ~3000 (**B**, **E** and **H**) and ~5000 (**C**, **F** and **I**).

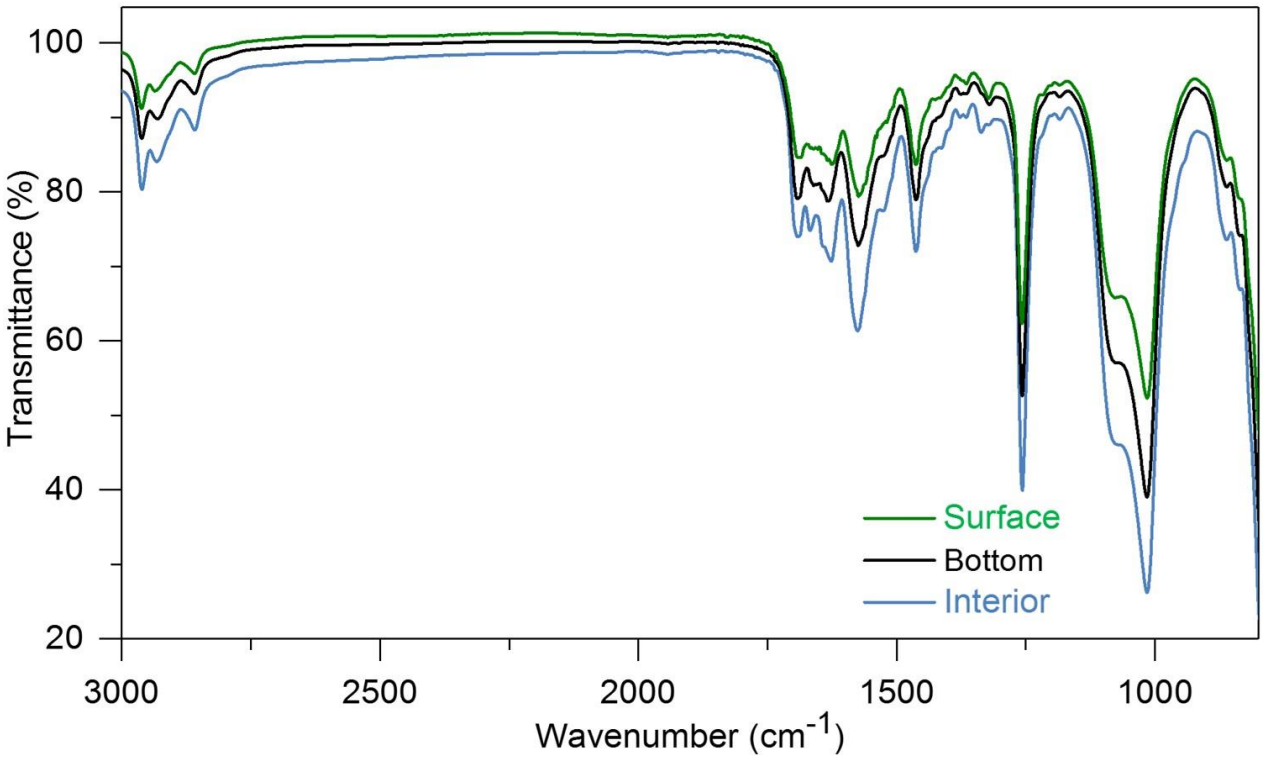

Fig. S3. Full ATR-IR spectra of different parts in DOSS coatings. Full ATR-IR spectra corresponding to Fig. 1A showing the comparison intensities of featured groups in the surface layer (green line), interior section (blue line) and bottom layer (black line) of DOSS coatings adhered on a substrate.

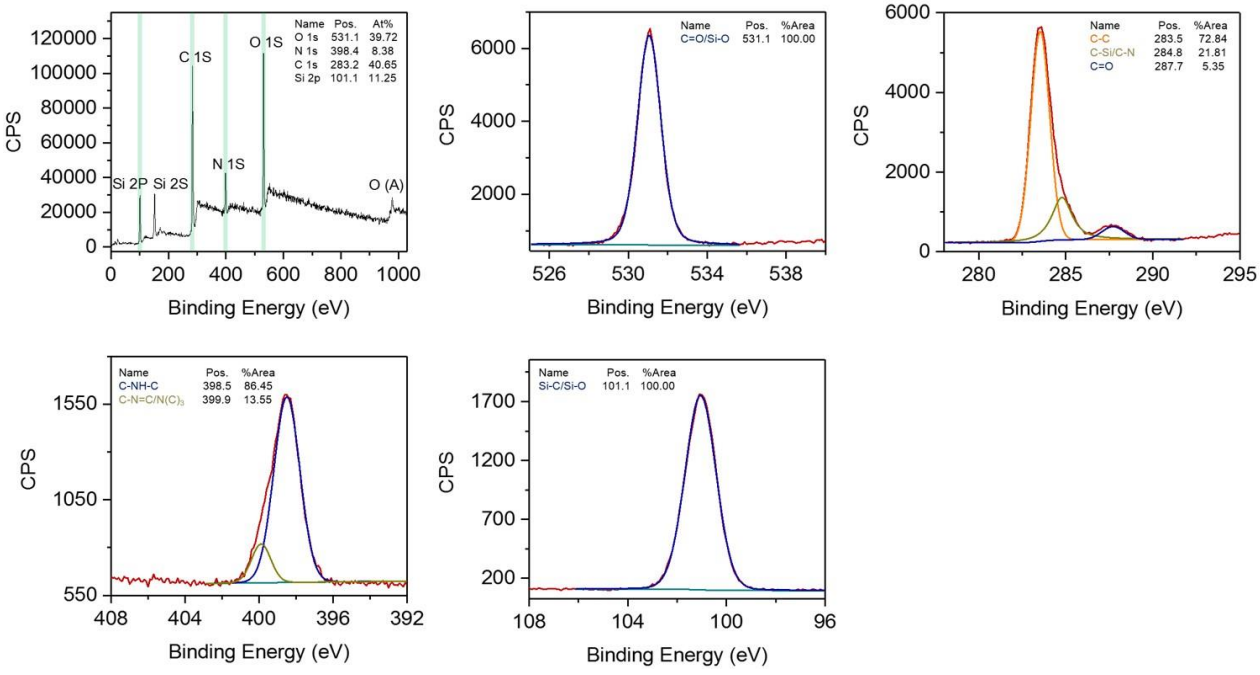

Fig. S4. Surface chemistry of the surface layer of DOSS coatings. Survey spectra and high-resolution spectra of the surface layer of DOSS coatings. The relative content of O 1s, C 1s, N 1s and Si 2p in the surface layer of DOSS coatings are 39.72%, 40.65%, 8.38% and 11.25%, respectively.

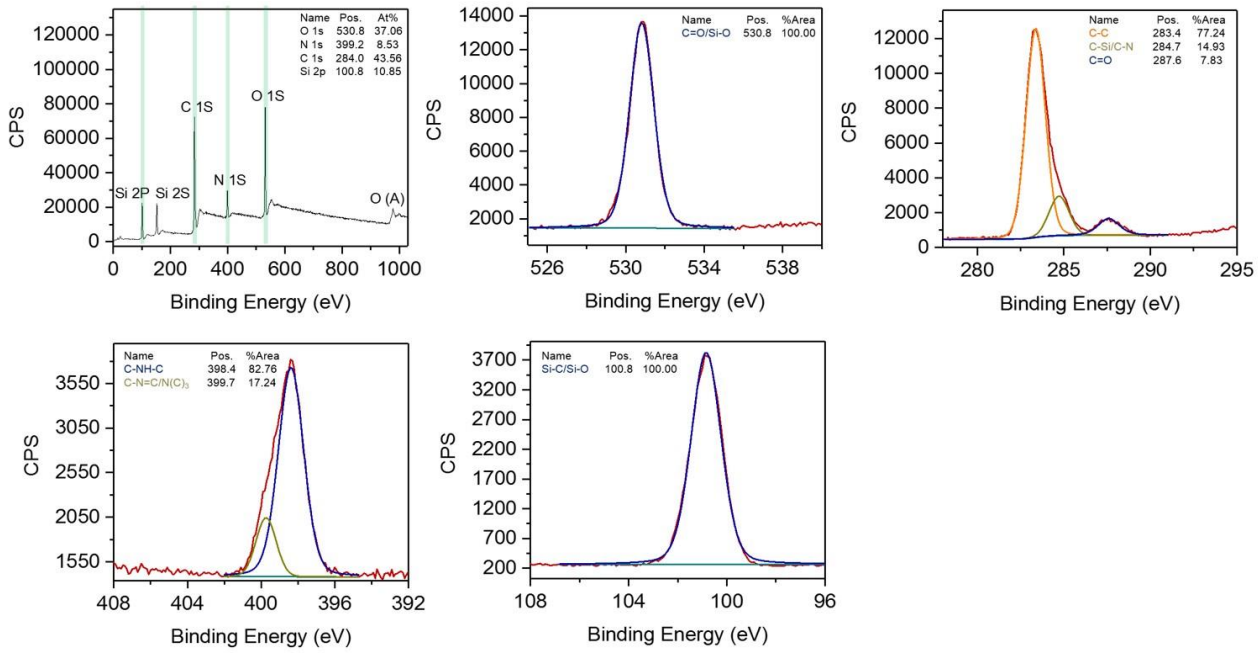

Fig. S5. Surface chemistry of the interior section of DOSS coatings. Survey spectra and high-resolution spectra of the interior section of DOSS coatings. The relative content of O 1s, C 1s, N 1s and Si 2p in the interior section of DOSS coatings are 37.06%, 43.56%, 8.53% and 10.85%, respectively.

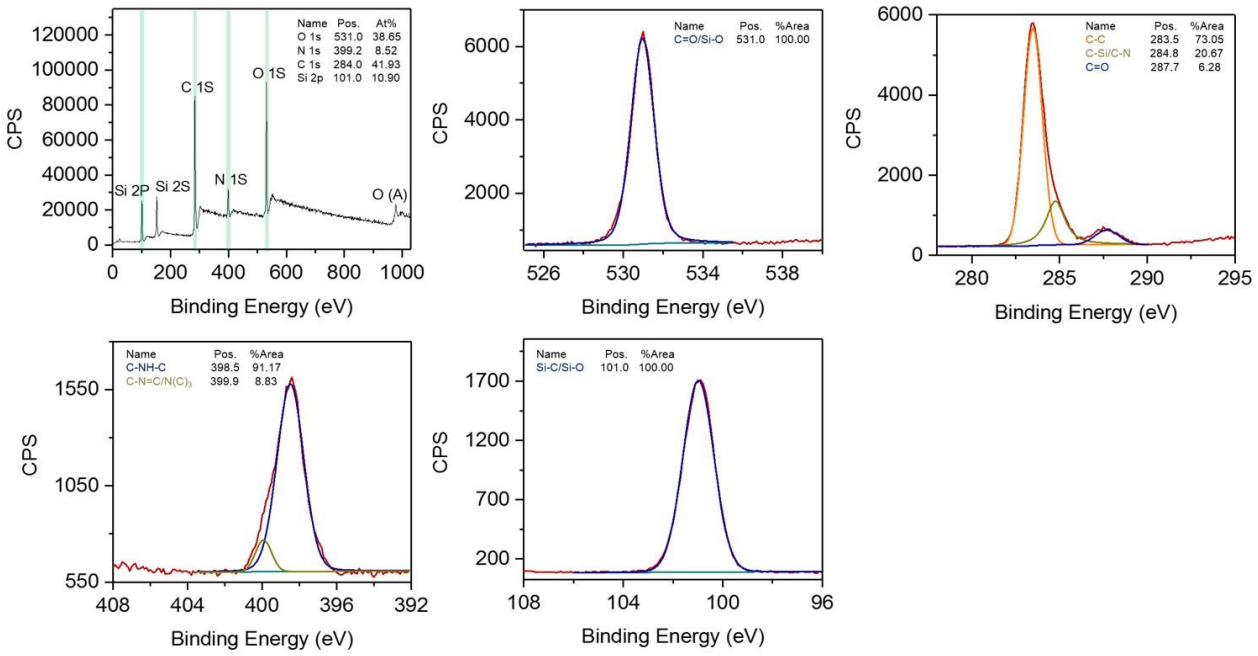

Fig. S6. Surface chemistry of the bottom layer of DOSS coatings. Survey spectra and high-resolution spectra of the bottom layer of DOSS coatings. The relative content of O 1s, C 1s, N 1s and Si 2p in the bottom layer of DOSS coatings are 38.65%, 41.93%, 8.52% and 10.90%, respectively.

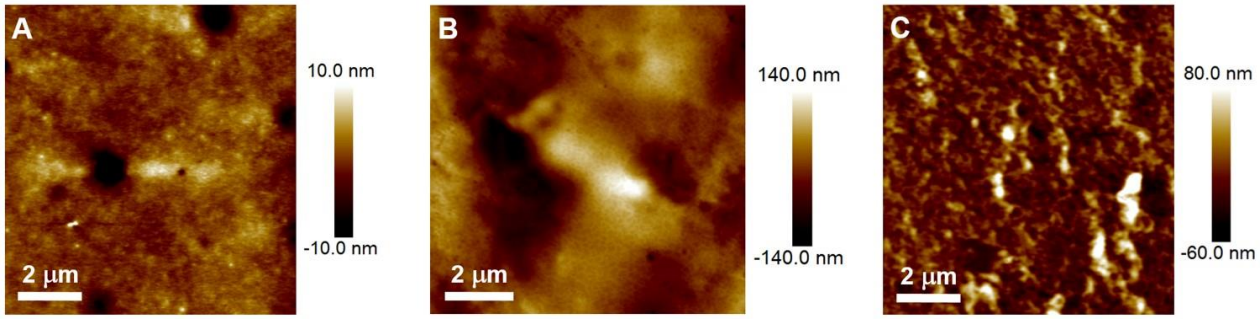

Fig. S7. Morphologies of different parts in DOSS coatings. Morphologies of the surface layer (**A**), interior section (**B**) and bottom layer (**C**) of the DOSS coating. The density of phase-separated domains grows sequentially from surface layer, interior section to bottom layer of the DOSS coating.

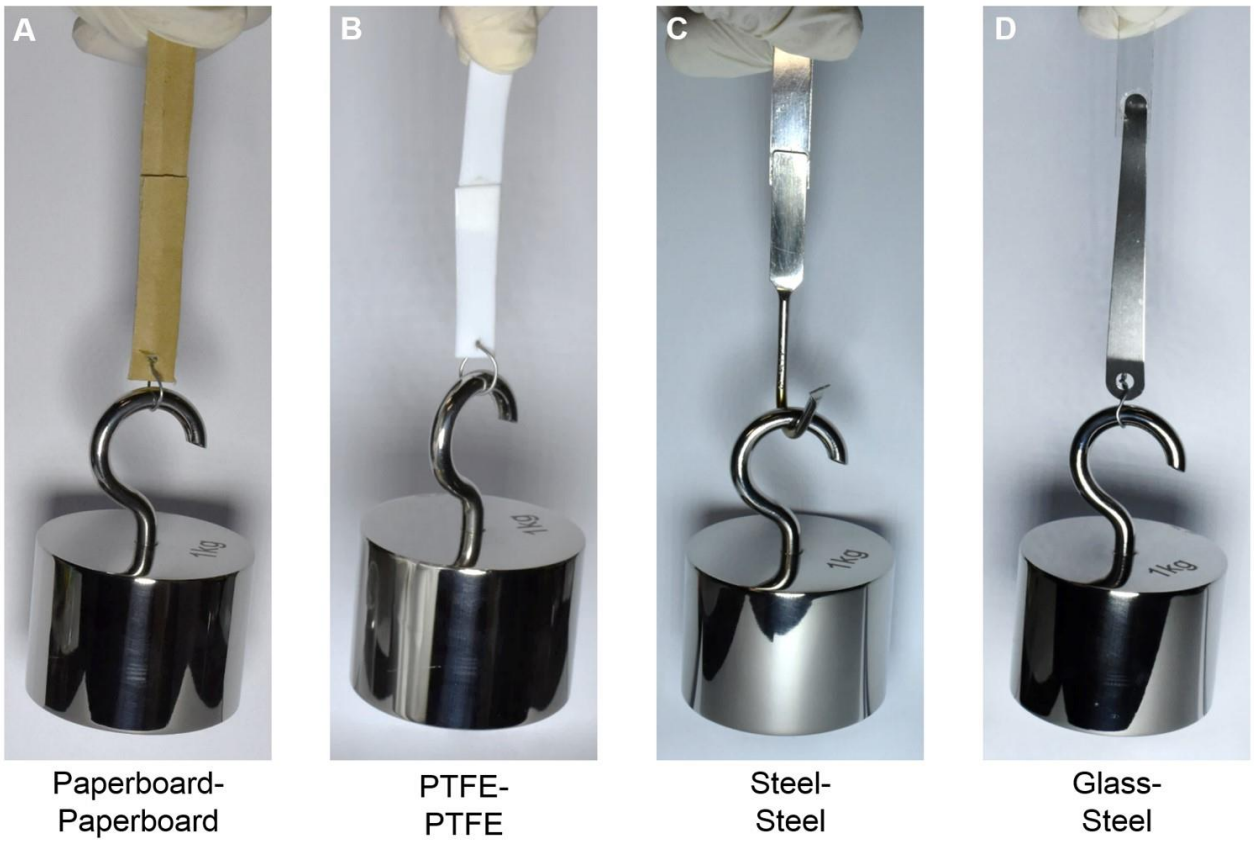

Fig. S8. Application of siloxane oligomer materials as adhesive materials. (**A** to **D**) Macroscopic adhesive behavior of siloxane oligomer materials on the surfaces of paperboard, PTFE, stainless steel and glass. All the adhesion areas are 1 cm^2. (Meijin Liu, City University of Hong Kong)

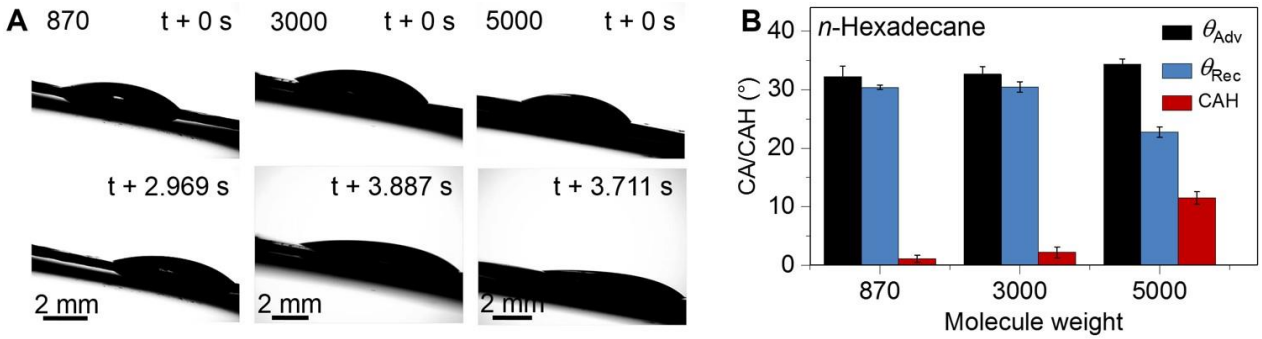

Fig. S9. Oil repellency and contact angle/CAH values of DOSS coatings with different MWs. (**A**) 10 μL *n*-hexadecane drops can slide away on all the three kinds of coatings, but the sliding velocity will decrease with the growth of the molecule weights. (**B**) Summaries of advanced contact angle, recede contact angle and CAH of DOSS coatings with different molecule weights. The CAH values will increase with the growth of molecule weight from ~870, ~3000 to ~5000, which implying that the coating prepared from DOSS with lower molecular weight demonstrated better oil-repellency properties.

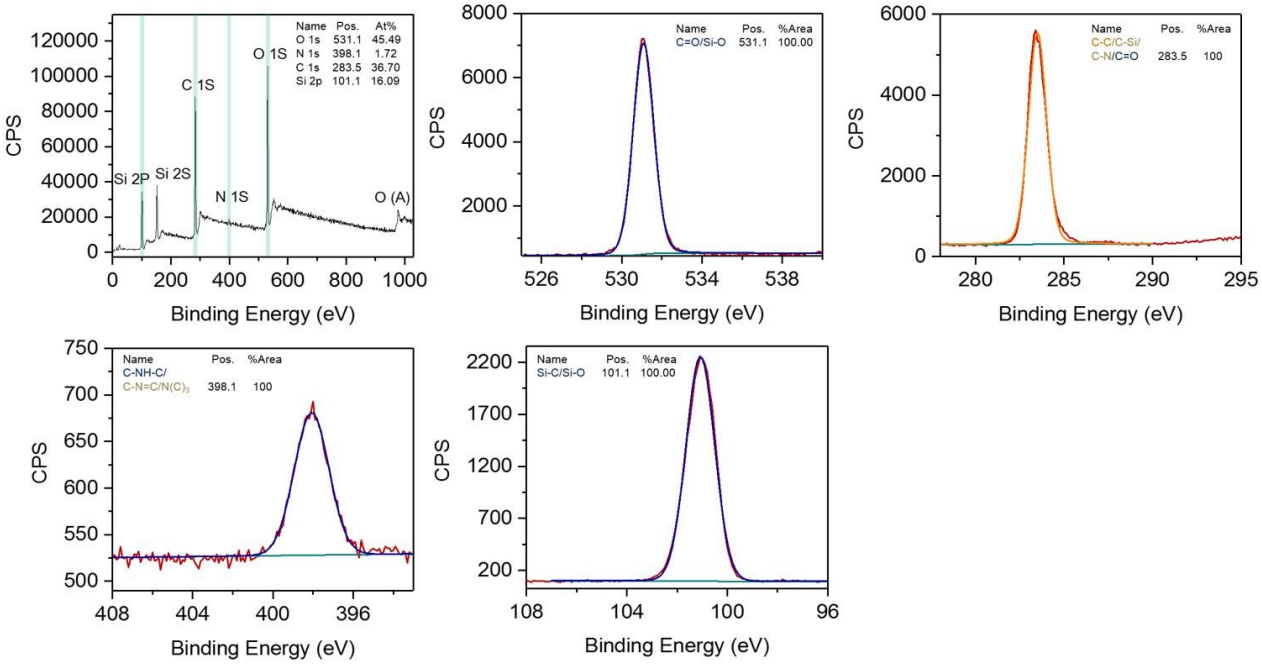

Fig. S10. Surface chemistry of the surface layer of DOSS coatings with MW of ~3000. Survey spectra and high-resolution spectra of the surface layer of DOSS coatings with molecular weight of ~3000.

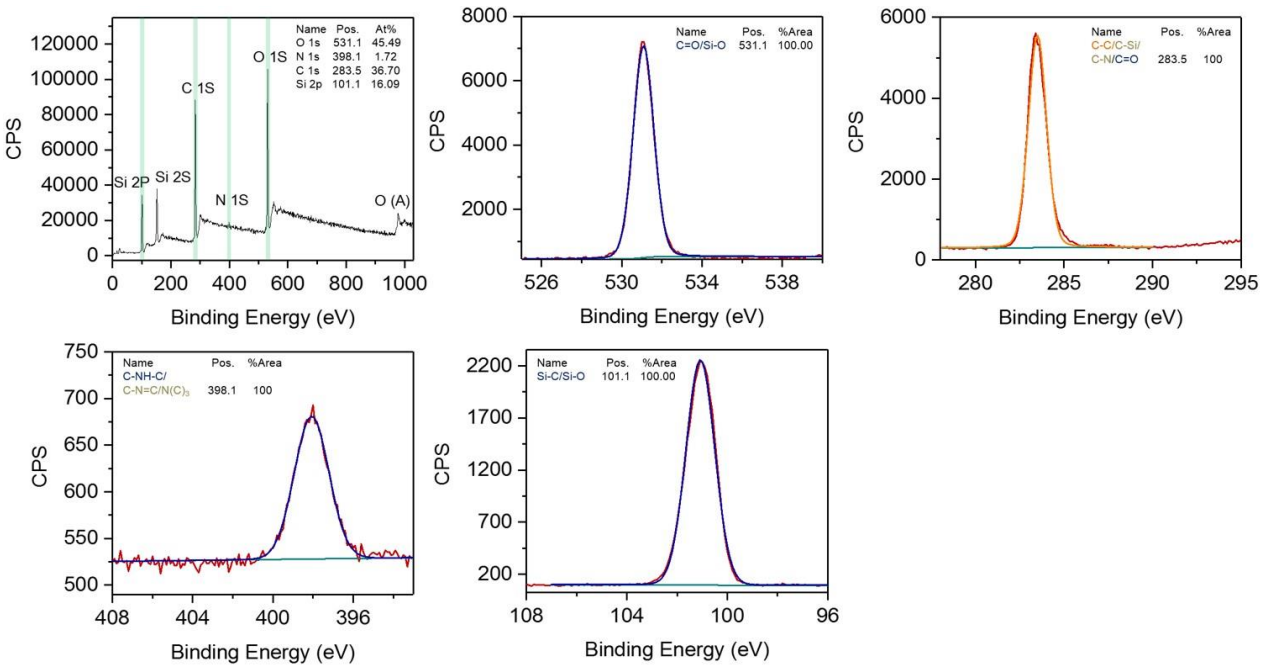

Fig. S11. Surface chemistry of the surface layer of DOSS coatings with MW of ~5000. Survey spectra and high-resolution spectra of the surface layer of DOSS coatings with molecular weight of ~5000.

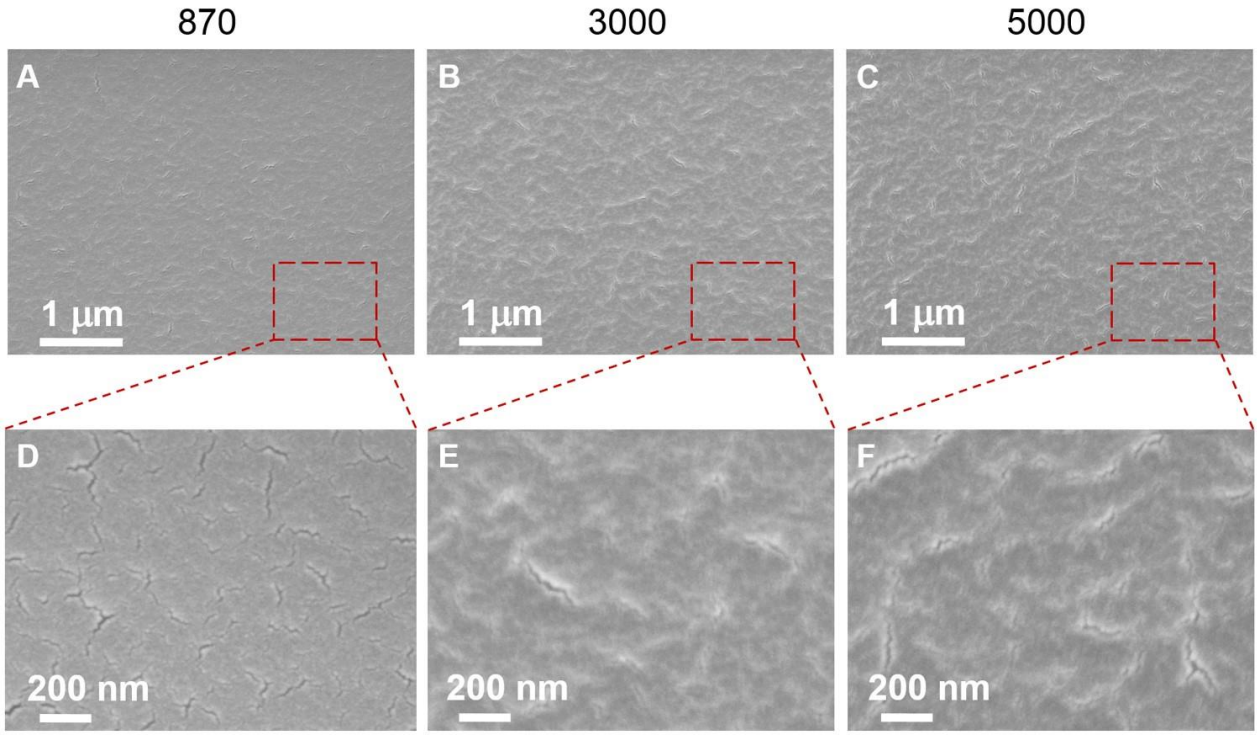

Fig. S12. Morphologies of the surface layers in DOSS coatings with different MWs. SEM images of the surface layer in the DOSS coatings with molecular weights of ~870 (**A** and **D**), ~3000 (**B** and **E**) and ~5000 (**C** and **F**).

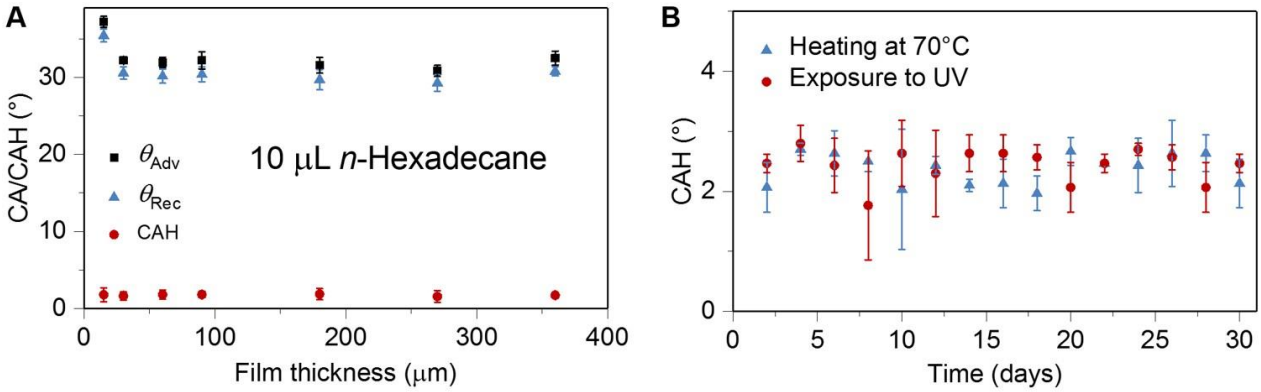

Fig. S13. Stability of DOSS coatings. (**A**) Effect of thickness on the coating oil-repellency. Droplets of 10 μL *n*-hexadecane can slide away from coatings with various thicknesses, demonstrating little differences in CAH. (**B**) Variation of CAH of *n*-hexadecane on the oil-repellent coatings sustained at 70°C in an oven (blue) and exposed to UV light (red).

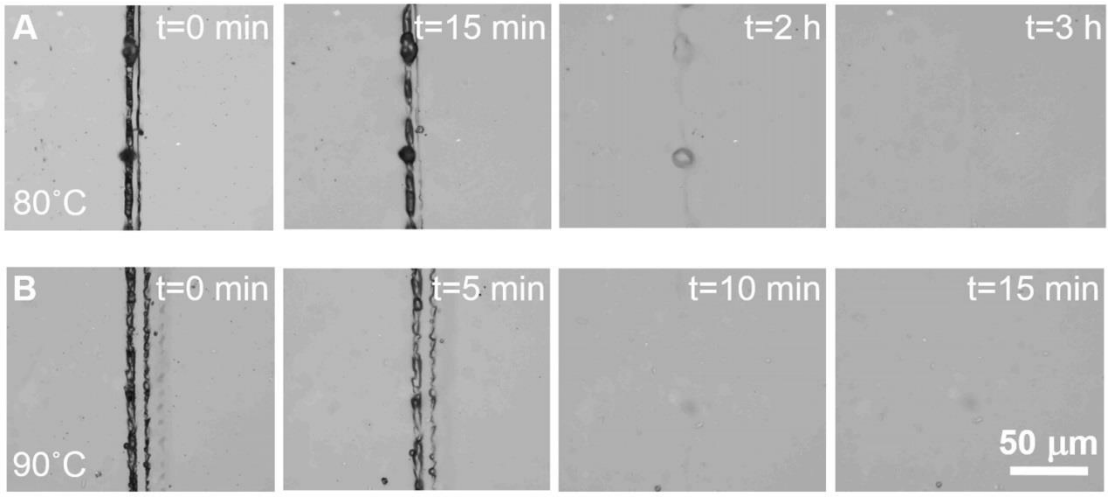

Fig. S14. Self-healing properties of the DOSS coatings (~870-MW siloxane oligomers) in different healing conditions. (**A**) Optical microscopic images of a damaged film after heating at 80˚C for 0 min, 15 min, 2 h and 3 h. (**B**) Optical microscopic images of a damaged film after heating at 90˚C for 0 min, 5 min, 10 min and 15 min. The coating can be healed after heating at 90˚C for 15 min or heating at 80˚C for 3 h.

Table S1. Mechanical properties of DOSS coatings with different MWs.

MW of H_2N-PDMS-NH_2	Break stress (MPa)	Break strain (mm/mm)	Young's modulus-Tensile test (MPa)	Storage modulus at 0°C (MPa)	Young's modulus-Indentation (MPa)
870	5.40 ± 0.23	0.56 ± 0.01	47.39 ± 1.03	264.48 ± 13.91	155.35 ± 10.27
3000	1.19 ± 0.18	0.54 ± 0.02	3.67 ± 0.32	30.67 ± 1.27	11.79 ± 1.41
5000	0.71 ± 0.06	0.53 ± 0.01	2.11 ± 0.21	0.38 ± 0.06	5.30 ± 0.29

Table S2. Assignment of the feature ATR–Fourier transform infrared bands of the spectra of the surface layer, interior section, and bottom layer of DOSS coatings corresponding to Fig. 2A and fig. S3.

	2962 $-CH_3$		2858 $-CH_2-$		1943 Siloxane		1668 Aggregated UPy motifs		1661 Dissociation UPy motifs
Surface	10.913		6.205		1.403		16.21		16.381
	1	:	0.568	:	0.129	:	1.485	:	1.501
							1	:	1.01
Interior	18.562		10.676		0.531		24.193		22.882
	1	:	0.575	:	0.028	:	1.303	:	1.232
							1	:	0.945
Bottom	12.787		6.811		0.182		18.174		19.159
	1	:	0.533	:	0.014	:	1.421	:	1.498
							1	:	1.054

Table S3. Assignment of the relative atom content of the surface layer, interior section, and bottom layer of DOSS coating (MW, 870) from the corresponding XPS spectra.

	Si 2p	C 1s	N 1s	O 1s
Surface	11.25%	40.65%	8.38%	39.72%
Interior	10.85%	43.56%	8.53%	37.06%
Bottom	10.90%	41.93%	8.52%	38.65%

Table S4. Assignment of the relative atom content of the surface layers of DOSS coatings with different MWs from the corresponding XPS spectra.

MW	Si 2p	C 1s	N 1s	O 1s
870	11.25%	40.65%	8.38%	39.72%
3000	16.09%	36.70%	1.72%	45.49%
5000	17.53%	36.26%	0.95%	45.26%